Vane rheometry of an aqueous solution of worm-like micelles

V.H. Rolón-Garrido, J. Pérez-González and L.A. Vega Acosta Montalban
Laboratorio de Reología, Departamento de Física, Escuela Superior de Física y Matemáticas,
Instituto Politécnico Nacional,
Apartado Postal 75-685, C. P. 07300, México D.F.

Recibido el 12 de junio de 2002; aceptado el 17 de septiembre de 02

The non-linear viscoelastic behavior of worm-like micelles in aqueous solution was analyzed in this work under non-homogeneous flow with a rotational vane rheometer. The system studied was a solution of cetylpyridinium chloride 100 mM/sodium salicylate 60 mM (CPyCl/NaSal) in triple distilled water. The use of the vane rheometer enables to reach higher shear rates than a cone and plate or Couette one because ejection of the sample and slip at the rotating surface are restricted. Thus, following this experimental procedure we show in this work, the complete flow curve for a micellar solution, including a hysteresis cycle and the upturn at high shear rates predicted by theories on constitutive instabilities and shear banded flow. We show in addition, the influence of time on the onset of flow instabilities and an experimental analysis of the flow stability in the low and high shear rate branches.

Keywords: Vane rheometry; micellar solutions; flow instabilities; top and bottom jumping.

El comportamiento viscoelástico no lineal de micelas tipo gusano en solución acuosa bajo flujo no homogéneo fue analizado en este trabajo mediante un reómetro rotacional de paletas. El sistema estudiado fue una solución de cetilpiridinio 100 mM/ salicilato de sodio 60 mM (CPyCl/NaSal) en agua tridestilada. El uso del reómetro de paletas permite alcanzar razones de deformación mayores que las obtenibles en cono y plato o Couette, ya que la expulsión de la muestra y el deslizamiento en la superficie giratoria están restringidas. Así, siguiendo este procedimiento experimental mostramos en este trabajo, la curva de flujo completa para un sistema micelar, incluyendo un ciclo de histéresis y el ascenso a altas razones de corte predicho por las teorías sobre inestabilidades constitutivas y flujo en bandas. Mostramos además, la influencia del tiempo sobre la aparición de inestabilidades de flujo y presentamos un análisis experimental de la estabilidad de flujo en los regímenes de baja y alta rapidez de deformación.

Descriptores: Reometría de paletas; soluciones micelares; inestabilidades de flujo; saltos superior e inferior.

PACS: 83.85.Cg; 83.60.Wc; 83.80.Qr

1. Introduction

Surfactants in solution self-assemble into molecular aggregates known as micelles, which can take different shapes depending on the concentration and ionic strength of the solution. Surfactants are not only of scientific interest, but have many practical uses as detergents, emulsifiers, viscosifiers, drag reducers and so on.

Long worm-like micelles act like "living polymers" because they are able to break and recombine themselves. At a high enough concentration, these micelles can entangle with each other; then, similar to ordinary linear polymers, they exhibit outstanding viscoelastic effects. Typical phenomena displayed by worm-like micellar systems include flow instabilities such as shear-induced structures and spurt.

Several authors have tried to capture the different phenomena observed in micellar systems through theoretical frameworks [1,2,3]. However, none of the available models is yet able to explain the whole range of possible phenomena in the non-linear rheology of micellar solutions. The latter, has been represented with a non-monotonic flow curve, which can be roughly divided into three regions as shown in Fig. 1.

The flow at low shear rates (region I) is generally stable and changes from Newtonian behavior to non-Newtonian shear thinning, then, at a critical shear stress (σ_t) the flow becomes unstable (region II). It has been suggested that the system splits into shear bands of low and high shear rates, whose volumetric fraction is determined by the "lever rule" [1], and that the high shear rate band is a shear induced nematic phase [4]. On the other hand, the flow in the high shear rate branch (region III) has been generally assumed to be stable [1]. If the shear stress is controlled, a hysteresis cycle is anticipated to occur for critical values, known as top (σ_t)

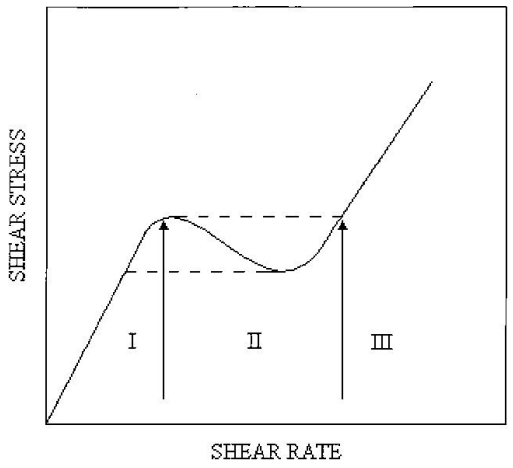

FIGURE 1. Schematic representation of a non-monotonic flow curve.

and bottom (σ_b) jumping. However, when the control parameter is the shear rate, a sigmoidal curve is expected, in which the maximum and minimum stresses correspond to σ_t and σ_b.

The study of the rheological behavior of micellar systems has been typically performed under homogeneous flow conditions. This arises in part from the lack of a constitutive equation able to describe the whole range of phenomena observed in micellar systems. However, the advantage of using homogeneous flow often disappears once the flow becomes unstable, since a mechanical instability changes the flow to a non-homogeneous one [1,5,6].

In this work we analyze the flow behavior of an aqueous solution of cetylpyridinium chloride 100 mM/sodium salicylate 60 mM (CPyCl/NaSal) under non-homogeneous flow with a rotational vane rheometer, which enables to reach higher shear rates than a cone-and plate one because ejection of the sample and slip at the rotating surface are restricted. Thus, although vane rheometer does not provide absolute viscosity values, it allows the investigation of the upturn regions in the non-monotonic flow curves associated to micellar solutions. Following this scheme, we show for the first time the complete flow curve for a worm-like micellar solution, including a hysteresis cycle.

2. Experimental

The system studied was an aqueous solution of cetylpyridinium chloride 100 mM/sodium salicylate 60 mM (CPyCl/NaSal) [7], which is able to form worm-like micelles, as well as developing shear bands and spurt under homogeneous and non-homogeneous flow, respectively, [8,9]. The CPyCl and NaSal (from Aldrich) had a purity of 98% and 99%, respectively, and were used as received.

Flow measurements were performed at 25 °C, which is above the Kraft temperature for this system. Fresh samples were used in each experiment to prevent pre-shearing history. A rotational Paar Physica rheometer USD 200 with the FL 100 vane-bob geometry in a measuring cup of 22.5 mm was used in this work under controlled torque and speed cycles. The vane consists of a shaft with six symmetrically spaced blades of 16 mm in length and 10 mm high. In addition, a cone and plate (25 mm radius and 2° angle) was used for calibration purposes.

When using the vane rheometer, values of torque (Γ) and angular velocity (Ω) are reported. Apparent shear rate and stresses can be determined through comparison with the Newtonian viscosity obtained under homogeneous flow; cone and plate data were used for this purpose as mentioned above. Γ and Ω are transformed to apparent shear stress (σ) and apparent shear rate ($\dot{\gamma}$) by means of a pair of constants obtained by superposition of the data from both rheometers as, $\sigma = K_\sigma \Gamma$ and $\dot{\gamma} = K_{\dot{\gamma}} \Omega$, with $K_\sigma = 20\text{m}^{-3}$ and $K_{\dot{\gamma}} = 1.129$ rev^{-1} [10]. Each type of experiment was repeated at least five times in order to ensure reproducibility within 2%.

3. Results and analysis

3.1. Cycles in shear rate and stress

Shear stress cycles were carried out in a stress range from 10 to 300 Pa. The stresses were chosen so that they were evenly spaced in a logarithmic scale. The number of data points in the increasing and decreasing parts of the cycle were the same, 100. In order to test the invariance of the flow curves, the time between consecutive points was varied in the range from 1 to 20 s. Two different curves comprising hysteresis cycles are present in Fig. 2 for 2 and 8 s between consecutive points, with the one corresponding to 2 s covering a wider area. An invariant curve was obtained when the time between consecutive points was 10 s or longer. In all cases a succession of instabilities was observed with increasing shear stress (see the arrows in Fig. 2). The instabilities started with a sudden increase in apparent shear rate leading to the high shear branch, followed by a Weissenberg effect and the motion of the fluid as a whole at shear rates beyond.

It is interesting to note that the hysteresis cycles are defined by two critical stresses, which are proposed here as the "top and bottom jumping" ones (σ_t and σ_b, respectively) as described by Spenley *et al.* [1]. For further experiments, the shear stress range was limited below the region in which the incipient Weissenberg effect was observed, *i.e.* up to 39.5 Pa, and using 10 s between consecutive points. New cycles obtained under controlled shear rate and stress conditions are shown in Fig. 3.

Several interesting characteristics can be observed in Fig. 3. First, note that all the data gathered during the increasing and decreasing parts of the cycles superpose at low shear rates suggesting that this flow regime is stable. Besides,

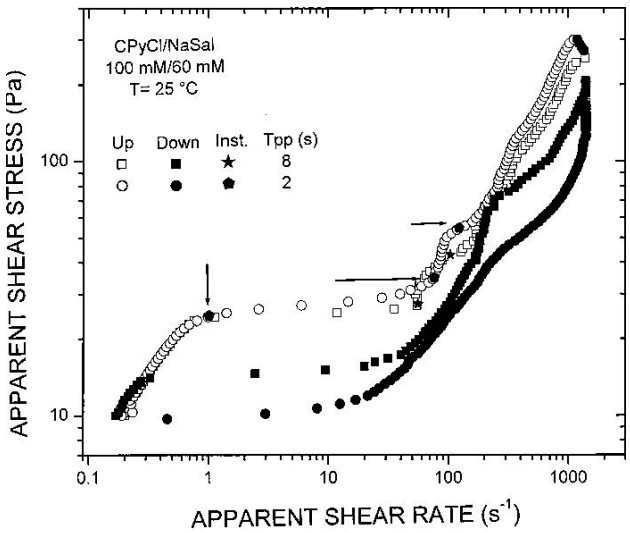

FIGURE 2. Cycles of controlled stress. Open symbols correspond to ascent (Asc.) and close symbols correspond to descent (Desc.). Pentagons and stars correspond to the onset of flow instabilities (Inst.).

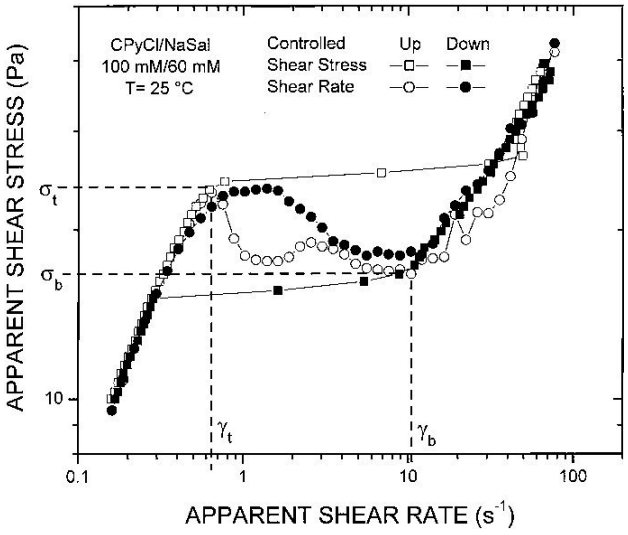

FIGURE 3. Cycles of controlled shear rate and stress.

the upturn occurring in the flow curve at high shear rates is also observed. The most interesting feature of Fig. 3 is, however, that the "top and bottom jumping" accompanied by hysteresis are clearly observed under both, controlled shear rate and stress, and that a true plateau in between is not present, in contrast to results by other authors [11]. While the controlled stress experiment produces a jump to the high shear rate branch and vice versa, the decreasing shear rate one produces the sigmoidal flow curve characteristic of a constitutive instability, which is reminiscent of critical phenomena as in the two fluid model of liquid helium [12]. In this view, the region in the middle of the sigmoidal depicts the coexistence of an isotropic phase and a structured in the fluid. These are remarkable results, since, to our knowledge, evidence of the hysteresis cycles and the whole sigmoidal flow curve characteristic of a constitutive instability had not been previously reported for micellar systems.

Besides providing an evidence for the "top and bottom jumping" in this solution, Fig. 3 suggests the mechanism for the onset of the instability during the cycles. When the shear stress or shear rate is increased up to σ_t or $\dot{\gamma}_t$ ("top jumping"), the fluid cannot longer sustain the deformation and shear banding occurs. As suggested by Lerouge and coworkers [13] this could be the result of a flow-induced structure with small sub-bands aligned in the flow direction making it non-homogeneous. This leads to a decrease in the average viscosity and a consequent increase in shear rate or decrease in stress depending on the controlled variable, torque or speed, respectively. On the other hand, when moving from high to low stress or shear rate up to σ_b or $\dot{\gamma}_b$ ("bottom jumping"), flow-induced shear bands start to disappear, leading to an increase in the fluid viscosity and a resulting decrease in shear rate or increase in stress. Thus, the process of nucleation and growth of any new phase is completely reversible under changes in shear rate or stress.

Hernández-Acosta *et al.* [14] and Méndez-Sánchez *et al.* [15] have suggested that there is a critical time for the onset of the unstable flow once σ_t has been reached. Such hypothesis was verified in this work using a shear stress cycle consisting of a slow ramp from 10 Pa up to σ_t, 23.6 Pa, which was kept constant during 1200 seconds. Then, the stress was decreased up to 10 Pa. The time between consecutive points in the ramps was 20 seconds and the number of points (26) to reach the critical stress was the same as in the previous experiments. The results of this experiment are shown in Fig. 4.

It can be observed that at the beginning of the upper plateau, there are data accumulating at around 0.7 s^{-1}as well as close to 25 s^{-1}, which means that there is a slow change in the apparent shear rate. In addition, a sudden increase in the flow rate is observed in between the above mentioned shear rates and beyond 25 s^{-1}. This is better seen in Fig. 5, in which the apparent shear rate has been plotted as a function of time once the critical stress is kept constant. After an overshoot due to fluid inertia, the flow stays in the high shear branch with variations in shear rate of the order of $\pm$ 6.5%.

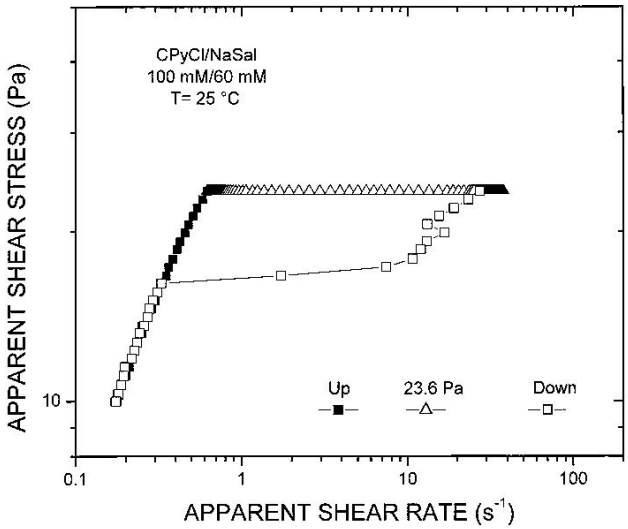

FIGURE 4. Cycles of controlled stress with a step at 23.6 Pa.

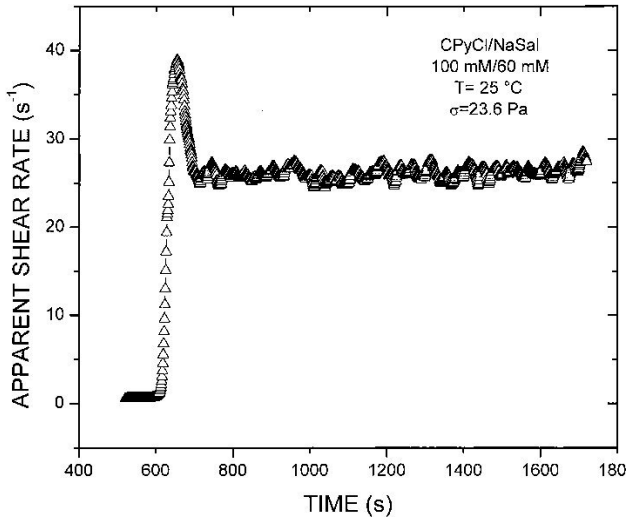

FIGURE 5. Apparent shear rate versus time in the step at 23.6 Pa.

Once the apparent shear stress is decreased the flow curve returns to the isotropic low shear rate branch, as was shown previously in Fig. 3. Here the question arises: why is there a need for a time of flow before the sudden increase in shear rate takes place?

The answer to the question could be based on the concept of creation and growth of the nematic phase that coexist with the initially isotropic one as suggested by Berret *et al.* [4]. There is a need for a critical time of flow to induce the critical orientation of the micelles to give rise to shear banded flow. The critical time in this work was estimated as of the order of 90 s (or $53\tau_R$, where τ_R is the longest relaxation time or Maxwell time), and it should be pointed out that no theory has considered it to explain the complex flow behavior of micellar systems.

3.2. Analysis of the flow stability in the low and high shear rate branches

The stability of the flow in the low and high shear rate branches was tested using parallel flow superposition. For this purpose a steady shear stress was imposed to the fluid along with a frequency swept in which the stress amplitude was 1 Pa. The results for shear stress values in the low shear rate branch are shown in Fig. 6.

It can be observed in all cases that the oscillatory evaluation was feasible, which proves the stability of the flow. This was not the case for shear stresses in the high shear rate branch, where the oscillatory experiment could not be performed. This result is in contrast with assumptions of flow stability in the high shear rate branch [1,6]. Additional proof of the unestable flow in such region should be provided, perhaps via optical methods.

It is interesting to observe from Fig. 6 that the fluid exhibits a Maxwell like behavior whose plateau modulus and relaxation time change with the steady shear stress. Plots of

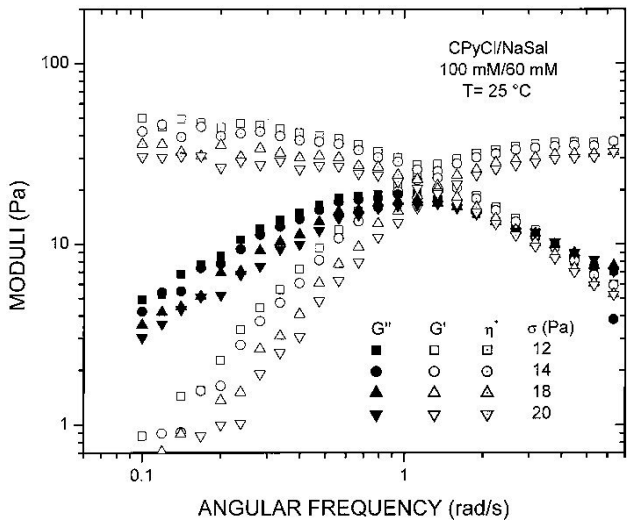

FIGURE 6. Superposition of oscillatory and shear flow.

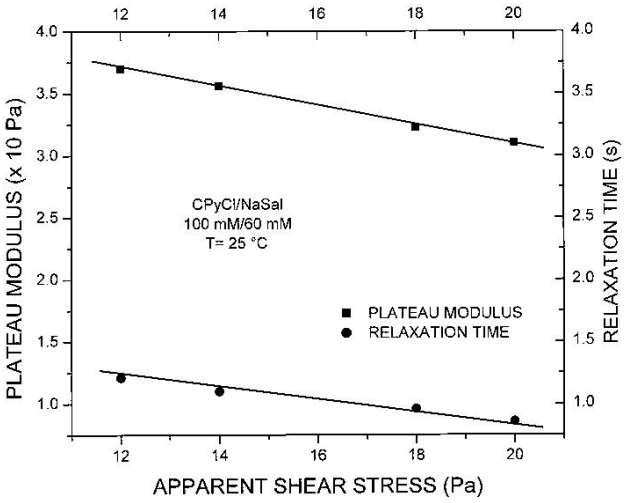

FIGURE 7. Plateau modulus and relaxation time as functions of the steady apparent shear stress.

the plateau modulus and relaxation time as functions of the apparent shear stress are shown in Fig. 7. It is seen that both physical quantities decrease linearly as the shear stress is increased, which reflects the change in the fluid structure leading to the unstable shear banding flow.

4. Conclusions

We have studied the non-linear rheology of a solution of cetylpyridinium chloride 100 mM/sodium salicylate 60 mM (CPyCl/NaSal) in triple-distilled water under non-homogeneous flow conditions with a vane rheometer, the main results are summarized below:

a) The complete flow curve characteristic of micellar systems suffering flow instabilities and shear banding is shown for the first time. Such a flow curve exhibits hysteresis and the top and bottom with a jump at the onset of the instability.

b) The influence of time on the onset of flow instabilities is shown. A critical time of the order of 90 s appears to be necessary to trigger the instabilities once the top critical shear stress is reached.

c) The flow in the low shear rate branch is stable, but this does not seem to be the case for the high shear one. Further studies are necessary to clarify this point.

Acknowledgments

This work was supported by CGPI-IPN (010565) and CONACyT (34971-U). J.P-G and L.A.V.A.M. are COFFA-EDI fellows. V.H.R.G. has scholarships from PIFI-IPN and CONACyT.

1. N.A. Spenley Yuan X.F., and M.E. Cates, *J.Phys. II* **6** (1996) 551.
2. P.D. Olmsted, O. Radulescu, and C.Y.D. Lu, *J. Rheol.* **44** (2000) 257.
3. F. Bautista, J.F.A. Soltero, J.H. Pérez-López, J.E. Puig and O. Manero, *J. Non-Newtonian Fluid Mech.* **94** (2000) 57.
4. J.F. Berret, D.C. Roux, and G. Porte, **4***J. Phys. II France* (1994) 261.
5. M.M. Britton and P.T. Callaghan, *J. Rheol.* **41** (1997) 1365.
6. J.F. Berret, *Langmuir* **13** (1997) 2227.
7. H. Rehage and H. Hoffmann, *Mol. Physics* **74** (1991) 933.
8. P.T. Callaghan, M.E. Cates, C.J. Rofe, and J.B.A.F. Smeulders, *J. Phys. II* **6** (1996) 375.
9. M.M. Britton, R.W. Mair, R.K. Lambert, and P.T. Callaghan, *J. Rheol.* **43** (1999) 897.
10. V.H. Rolón-Garrido Tesis de Licenciatura, Instituto Politécnico Nacional, México (2002).
11. C. Grand, J. Arrault, and M.E. Cates, *J. Phys. II France* **7** (1997) 1071.
12. G. Careri, *Order and Disorder in Matter*, (The Benjamin/Cummings Publishing Company, California, 1984).
13. S. Leoruge, J.P. Decruppe and J.F. Berret, *Langmuir* **16** (2000) 6464.
14. S. Hernández-Acosta, A. González-Alvarez, O. Manero, A.F. Méndez-Sánchez, J. Pérez-González, and L. de Vargas, *J. Non-Newtonian Fluid Mech.* **85** (1999) 229.
15. A.F. Méndez-Sánchez, M.R. López-González, V.H. Rolón-Garrido, J. Pérez-González, and L. de Vargas (to appear in *Rheol. Acta*, 2002).